Journal of Applied Polymer Science

Hydrophilic goethite nanoparticle as a novel antifouling agent in fabrication of nanocomposite polyethersulfone membrane

Masoud Rahimi,[1] Sirus Zinadini,[2] Ali Akbar Zinatizadeh,[2] Vahid Vatanpour,[3] Laleh Rajabi,[4] Zahra Rahimi[2]

[1]CFD Research Center, Department of Chemical Engineering, Razi University, Kermanshah, Iran
[2]Water and Wastewater Research Center (WWRC), Department of Applied Chemistry, Razi University, Kermanshah, Iran
[3]Faculty of Chemistry, Kharazmi University, Tehran 15719-14911, Iran
[4]Polymer Research Center, Department of Chemical Engineering, Razi University, Kermanshah, Iran
Correspondence to: S. Zinadini (E-mail: sirus.zeinaddini@gmail.com)

ABSTRACT: The goethite nanoparticle was used as a multifunctional additive to fabricate antifouling polyethersulfone (PES) nanofiltration membranes. The goethite/PES membranes were synthesized via the phase inversion method. The scanning electron microscopy (SEM) photographs showed an increase in pore size and porosity of the prepared membranes with blending of the goethite. The static water contact angle measurements confirmed a hydrophilic modification of the prepared membranes. With increase in the goethite content from 0 to 0.1 wt %, the pure water flux increased up to 12.7 kg/m^2 h. However, the water permeability decreased using high amount of this nanoparticle. Evaluation of the nanofiltration performance was performed using the retention of Direct Red 16. It was observed that the goethite/PES membranes have higher dye removal capacity (99% rejection) than those obtained from the unfilled PES (89%) and the commercial CSM NE 4040 NF membrane (92%). In addition, the goethite/PES blend membranes showed good selectivity and antifouling properties during long-term nanofiltration experiments with a protein solution. © 2016 Wiley Periodicals, Inc. J. Appl. Polym. Sci. **2016**, *133*, 43592.

KEYWORDS: applications; membranes; nanoparticles; nanowires and nanocrystals

Received 14 November 2015; accepted 4 March 2016
DOI: 10.1002/app.43592

INTRODUCTION

Colored wastewater is a consequence of batch processes in the dye manufacturing or the dye-consuming industries (such as textile processing industry). Large amounts of the colored wastewater discharged by the textile industries have caused a detrimental effect on the environment.[1] Therefore, in order to reduce the environmental impacts, discharge limits imposed on textile mills are becoming ever more stringent and are forcing plant managers to upgrade their waste treatment systems. In addition, because of decreasing natural water resources and increasing water price in future, water reuse could be a promising strategy for industries sustainability. The most wide treatment methods applied to treat and recycle of the colored wastewater comprise biological treatment, precipitation, coagulation/flocculation, flotation, oxidation, and adsorption.[2–6] However, because of recalcitrant organic compounds and sometimes even toxicity of components, an advanced treatment technology as well as complete decolorization is necessary.[7] For this purpose, nanofiltration membrane could be an efficient separation method because of inefficiency of the conventional treatment systems.[8]

Nanofiltration (NF) has been recognized as a filtration method placed between ultrafiltration (UF) and reverse osmosis (RO). It is much more efficient than UF in terms of rejection and it faces lesser fouling problems than RO. However, a limitation of more extensive application of nanofiltration membrane process is the significant flux decline that occurs during membrane filtration as a result of fouling.[8] Deterioration of flux can be caused by the accumulation and adhering of organic and inorganic species inside membranes pores. It can cause a higher operating pressure requirement, an increase in operating costs, restricted recoveries, repeated chemical cleaning, and shortening of membrane life.[9] Therefore, it is important to develop advanced antifouling membrane that have high resistance to fouling and flux decline.

In literature, it is approved that fouling resistance will be decreased by increasing membrane hydrophilicity.[10–16] This can be attributed to the hydrophobic nature of organic matter and

many other foulants. In order to improve the membrane hydrophilicity and fouling reduction, many attempts have been carried out including; adding grafting hydrophilic monomers on the membrane top layer,[12] blending an amphiphilic terpolymer in the polymer matrix,[13] functionalization of the polymer,[14] coating substrate membrane with hydrophilic polymer,[15] etc. Although permeation flux by employing these techniques have been improved, the efforts are not still sufficient to obtain adequate diminish of membrane fouling.

In the last decade, considerable scientific efforts have been performed for using nanotechnology in membrane science to improve their synergistic effects on water and wastewater treatment. Using nanoparticles for preparation of hybrid inorganic–organic nanocomposite membranes, mixed matrix membranes (MMMs), have been recently reported from many research groups to improve performance of membranes.[16] Appropriate interactions between nanoparticles surface and polymer chains and/or solvents during membrane preparation can lead to membranes with desirable structure and appropriate performance. Also, mitigation of membrane fouling caused by hydrophilic functionalized nanoparticles is another target in MMMs.[16]

In recent years, use of nanoparticles in the manufacturing process of nanocomposite polymeric membranes especially for their flux enhancement and fouling reduction has received a lot of attention.[17] Kim and Van der Bruggen[16] reviewed the use of nanoparticles in polymeric and ceramic membrane structures. Many kinds of inorganic nanoparticles, such as nano-TiO_2, nano-Al_2O_3, silica, and sliver nanoparticles, etc. can be used for the modification of different polymeric membranes besides PES membrane. Most of these nanoparticles can be used for modifying PES membrane. For instances, polyvinylidene fluoride membranes incorporated with silica nanoparticles showed higher temperature endurance, higher selectivity, and higher diffusivity.[18] Chitosan/zinc oxide nanoparticle membranes exhibited good mechanical properties and high antibacterial activities.[19] Polysulfone membranes incorporated with silica nanoparticles exhibited enhanced gas permeability.[20] Polyethersulfone (PES)/aluminum oxide membranes exhibited lower flux decline, higher porosity and pseudo steady-state permeability.[21] Moreover, poly benzimidazole/silica nanoparticles membranes showed higher permeability and selectivity in gas separation than the unfilled membranes.[22]

Recent work has begun to take advantage of iron's potential, and use it in membrane separation processes. However, high reactivity of the iron metal limits its use as pure metal nanoparticles. Therefore, in most cases, iron compounds instead of pure iron nanoparticles were incorporated into the polymeric membranes. Hosseini *et al.*[23] have shown that addition of the proper amounts of magnetic iron-nickel oxide particles can improve performance of polyvinylchloride-based heterogeneous ion exchange membranes. Harman *et al.*[24] have examined removal of natural organic matter (NOM) from wastewater using ceramic membranes that coated with iron and aluminum oxide coating layer. Daraei *et al.*[25] have synthesized mixed matrix polymeric membrane from PES and self-produced polyaniline/iron oxide (PANI/Fe_3O_4) nanoparticles by the phase inversion method. In that study, it was found that the blended membranes has better antifouling performance and Cu (II) ion removal capacity is more than unfilled (PES) membrane.

Goethite is an iron oxyhydroxide with formula of α–FeO(OH), which has orthorhombic crystal and yellowish color.[26] It is a mineral oxide found in soil and other low-temperature environments. The surface of goethite nanoparticles is covered with hydroxyl (-OH) groups.[27]

The presence of extra hydroxyl groups on the surface of nano-goethite particles was the main aim of using it in fabrication of NF MMM, which could enhance membrane hydrophilicity and surface properties. As a result, it can reduce fouling of the prepared MMMs.

To our knowledge, limited studies employed nano-goethite for fabricating mixed matrix PES nanofiltration membranes. Zhang *et al.*[28] have reported the preparation of membrane composed of α-FeOOH and poly(vinyl alcohol) (PVA) as a proton exchange membrane (PEM) for fuel cell application. Also, the goethite was used in the synthesis of ceramic membranes.[29]

This research, aims to study the preparation of a novel PES MMM by blending nano-sized goethite particles to improve their hydrophilicity and fouling resistance. The nano-goethite particles were synthesized, characterized, and used as nano-filler in the fabrication of nanocomposite PES membrane by the wet phase inversion method. The effect of nano-sized α-FeOOH at different concentrations in casting solution on morphology, permeability properties, dye rejection, hydrophilicity, and antifouling performance of the membranes was investigated. Morphology and structure of each membrane were analyzed using scanning electron microscope (SEM). Membrane hydrophilicity was also determined using contact angle measurements. The performances of the prepared membranes were investigated by measuring pure water flux, Direct red 16 rejection and milk powder solution permeation tests. The performance of the prepared nanocomposite membranes was compared with commercial CSM NF membrane.

MATERIALS AND METHODS

Chemicals

All chemicals used in the experiments were of reagent grade. PES (Ultrason E 6020P) and dimethylacetamide (DMAc) as solvent were purchased from BASF Co., Germany. Polyvinylpyrrolidone (PVP) with 25,000 g/mol molecular weight, KOH, and iron nitrate were obtained from Merck to synthesize goethite nanoparticle. The NE 4040-90 membrane manufactured by CSM, South Korea, was used in this study. The used membrane was a thin-film polyamide composite membrane in spiral wound element configuration. The module was opened and the flat sheet membrane was used in the experiments. Distilled water was used throughout this study.

Synthesis of Goethite Nanoparticle

The goethite nanoparticle was synthesized in the laboratory. Firstly, 4.85 g of Fe $(NO_3)_3.9H_2O$ was dissolved in 50 mL distilled water by continuous stirring. Then, the potassium

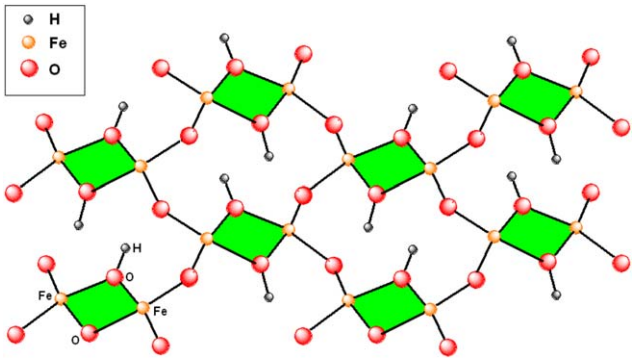

Figure 1. The crystal structure of goethite nanoparticles. [Color figure can be viewed in the online issue, which is available at wileyonlinelibrary.com.]

hydroxide solution (2.73 g in 10 mL H_2O) was added very slowly to the iron solution with vigorous stirring. The pH of resulting mixture was adjusted to 12 using KOH solution. Then, the mixture was subjected to mixing in the ultrasonic bath (SONREX Digite C Ultrasonic bath, DT52 H model, made by Bandelin Company, Germany) for 30 min at the temperature of 25 °C. The resulted precipitates were filtered and washed by distilled water and were kept in the oven at 100 °C for 75 min for drying. Figure 1 shows the crystal structure of functionalized goethite covered with large number of OH groups.

Fabrication of Goethite Nanoparticle/PES Mixed Matrix Nanofiltration Membrane

Asymmetric goethite-blended PES nanofiltration membranes were prepared via the immersion phase inversion method. In brief, the precise amounts of goethite nanoparticle (0.01, 0.05, 0.1 wt % related to total polymer solution) were dispersed in DMAc as a solvent by sonication for about 20 min to improve the homogeneity. Afterwards, the appropriate amounts of PES (21 wt %) and PVP (1 wt %) were dissolved in dope solution by continuous stirring for 24 h. The PVP was used as a pore forming to promote the yield of pores in the coagulation process. It should be mentioned that the membranes marked as 0.1 wt %, refer to membranes prepared in a casting solution in which the amount of the goethite nanoparticle with respect to the casting solution of PES and DMAc was 0.1 wt %. Finally, the prepared homogenous polymer solution was again sonicated for 20 min to remove air bubbles and efficient dispersing of the goethite in the polymer matrix. Consequently, the solutions were casted using self-made casting knife with 250 μm thickness on glass plate and immediately moved to distilled water as a nonsolvent bath for immersion at room temperature without any evaporation. After primarily phase separation and membrane formation, the membranes were stored in fresh distilled water for 24 h to guarantee the complete phase separation. Finally, for drying, the membranes were sandwiched between two sheets of filter papers for 24 h at room temperature.

Characterization of the Prepared Membranes

The Fourier transform infrared spectroscopy (FT-IR, Bruker alpha, German) spectra were recorded between 400 and 4000 cm^{-1} with KBr pellets at room temperature to detect chemical compositions of the goethite nanoparticle. The surface and cross-sectional morphology of the blended membranes were examined using SEM (Philips-XL30, The Netherland) with an accelerating voltage of 25 kV. The membranes were cut into small pieces and cleaned with a filter paper. The cross-section samples were obtained by fracturing the membranes after cooling in liquid nitrogen for 60–90 s. The dried frozen fragments were gold sputtered for producing electric conductivity.

Overall Porosity and Mean Pore Size

The overall porosity (P_r) was determined by gravimetric method, as defined in the following equation[18]:

$$P_r = \frac{m_w - m_d}{\rho\, SL} \tag{1}$$

where m_w is the weight of the wet membrane; m_d is the weight of the dry membrane; S is the membrane effective area (m^2), ρ is the water density (0.998 g/cm^3), and L is the membrane thickness (m).

In addition, in order to determine the membrane mean pore radius (r_m), Guerout–Elford–Ferry equation [eq. (2)] on the basis of the pure water flux and porosity data was utilized[10,11]:

$$r_m = \sqrt{\frac{(2.9 - 1.75P_r) \times 8\eta LQ}{P_r \times S \times \Delta P}} \tag{2}$$

where η is the water viscosity (8.9×10^{-4}Pas), Q is the volume of permeate pure water per unit time (m^3/s), and ΔP is the operation pressure (0.4 MPa).

Zeta Streaming Potential Measurement

The separation mechanism of nanofiltration membranes is typically explained in terms of charge and sieve effect.[30] Therefore, information about the surface charge will be valuable in explaining the results. Zeta potential of the prepared membranes was determined by streaming potential method along the membrane surface using an EKA Electro Kinetic Analyzer instrument (Anton Paar, Austria). In the streaming potential method, movement of an electrolyte solution through a capillary system creates a streaming potential where the relation with the zeta potential of the capillaries is given by Smoluchowski-Helmholtz approach[31–33]:

$$\zeta = \frac{dU}{dp} \frac{\eta}{\varepsilon . \varepsilon_\circ} \frac{H}{Q . R} \tag{3}$$

where ζ is zeta potential, dU/dp is slope of streaming potential versus pressure, ε_o is permittivity, ε is dielectric constant of electrolyte, H is length of the capillary system, Q is cross-sectional area of the capillary system, and R is AC resistance of cell using electrolyte solution. According to Fairbrother and Mastin approach,[34] for electrolyte concentrations greater or equal to 10^{-3} M, the ratio $H/Q.R$ in eq. (3) can be replaced by K_B, the specific electrical conductivity of the electrolyte solution outside the capillary system.

Zeta potential measurements were performed with a clamping cell. Prior to zeta potential measurements, the membranes were washed by circulating deionized water across the membrane surface for 20 min. Measurements were made with 0.001 M KCl electrolyte solution. During the measurements, pH of solutions varied in the range of 3–8 by adding 0.1 N solutions of NaOH

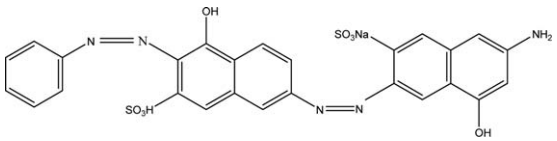

Figure 2. Chemical structure of direct red 16 dye.

and HCl. Because of construction design of clamping cell, the measurements were made by firmly pressing the test surface against a PMMA grooved spacer. Therefore, the zeta potential of the sample was calculated according the following relation:

$$\zeta_s = 2\zeta_{tot} - \zeta_{PMMA} \quad (4)$$

where ζ_{tot} is the zeta potential of sample plus PMMA, ζ_{PMMA} is the zeta potential of PMMA, and ζ_s is the net zeta potential of the sample.

Filtration Performance

The permeate flux, separation and fouling tests of the goethite embedded nanofiltration membranes were carried out in a dead-end cell (200 mL volume) with a membrane surface area of 12.56 cm^2 that equipped with magnetic stirrer. The cell was fitted with a pressure gauge and pressurized with nitrogen gas to force the liquid through the membrane. The feed solution was stirred at the rate of 300 rpm. The trans-membrane pressure (TMP) was adjusted at 6 bar for 30 min to compact the membrane. Then, the pressure was reduced to the operating pressure of 4 bar. The water flux $j_{w,1}$ (kg/m^2 h) was calculated using the following equation:

$$j_{w,1} = \frac{M}{A\Delta t} \quad (5)$$

where M (kg) is the weight of permeated water, A (m^2) is the membrane area, and Δt (h) is the permeation time. The experiments were carried out at 20 ± 1 °C and the average of three replicates was depicted in figures.

Antifouling Experiments

In order to investigate fouling resistance of the prepared membranes, milk powder solution at concentration of 8000 mg/L as a good fouling agent was used. One of the main applications of UF and NF membranes are in dairy industries. Therefore, we used milk powder as a test solution to provide similar medium. After measuring pure water flux, the stirred cell was rapidly refilled with the foulant solution. Then, the flux for milk powder solution j_p (kg/m^2 h) was measured based on the water quantity permeating the membranes at 4 bar for 90 min. The fouled membrane was immersed in distilled water for 15 min to remove temporarily attached foulants to the membrane surface. The cleaned membrane was immediately placed in cell without drying and then the pure water flux was measured again for 60 min as $j_{w,2}$. Subsequently, the flux recovery ratio (FRR) of the membranes was calculated according to the following equation:

$$FRR = \left(\frac{j_{w,2}}{j_{w,1}}\right) \times 100 \quad (6)$$

In addition, fouling resistances including total fouling resistance (R_t), reversible fouling resistance (R_r), and irreversible fouling resistance (R_{ir}) were determined for deeper investigation of antifouling properties of the prepared membranes. The equations are as follows[12]:

$$R_t(\%) = \left(1 - \frac{j_p}{j_{w,1}}\right) \times 100 \quad (7)$$

$$R_r(\%) = \left(\frac{j_{w,2} - j_p}{j_{w,1}}\right) \times 100 \quad (8)$$

$$R_{ir}(\%) = R_t - R_r \quad (9)$$

Because the main application of the prepared membranes in this work was the dye removal, the FRR of the membranes was also examined by the dye filtration.

Dye Removal Experiments

In the present study, Direct red 16 was selected as a dye containing azo group. Chemical structure of this dye is indicated in Figure 2. In order to evaluate the dye removal efficiency of the prepared membranes, filtration experiments were performed in the dead-end filtration cell for 120 min with driving force of 4 bar. In every run, 200 mL of synthetic dye solution (30 mg L^{-1}), which is within the range of typical concentration in textile wastewaters, was used and the flux and rejection were calculated from eqs. (5) and (10).[35] UV–Vis spectrophotometer (JENWAY 6320D) at 526 nm was employed for dye concentration determination. The calibration standard curves with $R^2 = 0.999$ was obtained. The following equation was used for assessment of dye removal (R) percent:

$$R(\%) = \left(1 - \frac{C_p}{C_f}\right) \times 100 \quad (10)$$

where C_f and Cp are dye concentration (mg/L) in feed and permeate, respectively.

RESULTS AND DISCUSSION

Characterization of Goethite Nanoparticle

The FT-IR spectrum of goethite nanoparticle is shown in Figure 3. The band closed to 3369 cm^{-1} was assigned to the H-O-H vibration. This band was a typical mode of nonstoichiometric hydroxyl units (excess water) in the goethite structure. This type of hydroxyl units can be incorporated into goethite structure

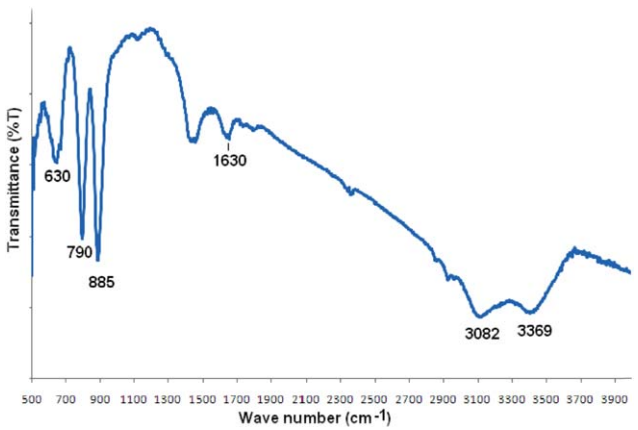

Figure 3. FT-IR spectrum of the synthesized goethite nanoparticle. [Color figure can be viewed in the online issue, which is available at wileyonlinelibrary.com.]

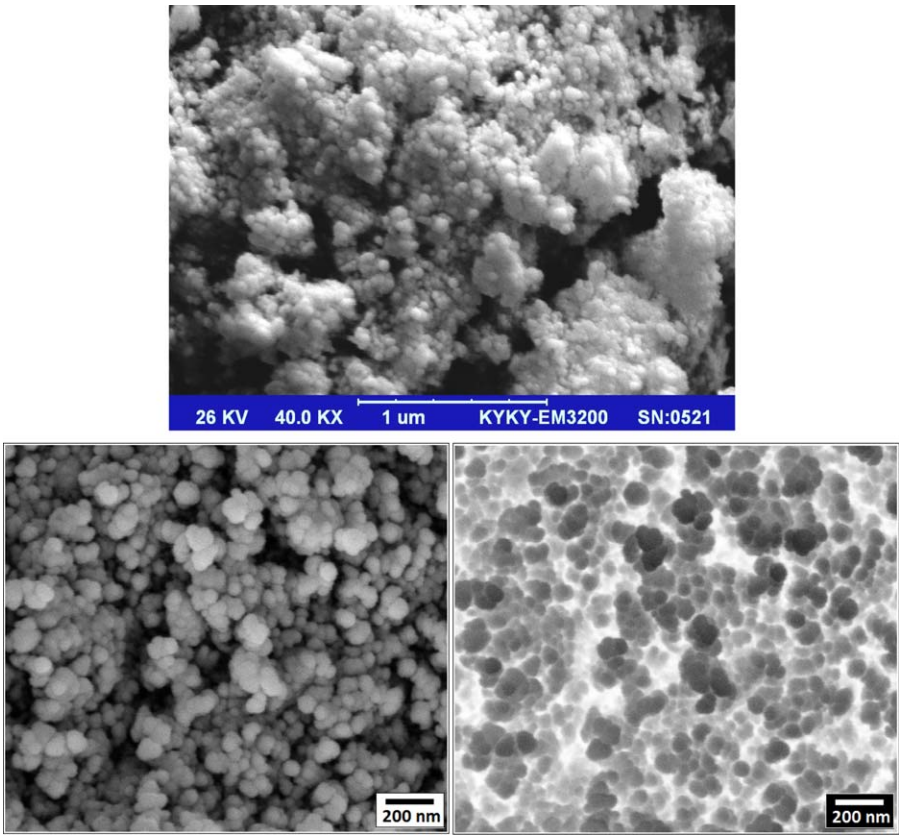

Figure 4. SEM image of the synthesized goethite nanoparticle with two resolutions. [Color figure can be viewed in the online issue, which is available at wileyonlinelibrary.com.]

and are adsorbed onto the crystal surface during the process of synthesis. The band at 1630 cm^{-1} was assigned to the water bending vibration. The band at 630 cm^{-1} was assigned to the Fe-O vibration. Strong absorption bands at 790 and 885 cm^{-1} caused by the in-plane bending of surface hydroxyl of Fe-OH-Fe were similar to those reported in literature. The intensity of the IR band of Fe-OH-Fe in-plane bending at 885 and at 790 cm^{-1} was in the order of the original goethite.[36,37]

Figure 4 presents the SEM images of the synthesized goethite nanoparticle. It is obvious that the synthetic goethite, α-FeOOH, has sphere form, ranging from 30 to 50 nm that can improve surface properties of the prepared membranes.

Characterization of Fabricated Nanofiltration Membranes

Morphology. The SEM images of the prepared membranes with different concentrations of the goethite nanoparticles with two magnifications are presented in Figure 5. These images clearly provide the visual information about cross-section of the prepared membranes. All of the membranes exhibited an asymmetric morphology with a dense top-layer and a porous finger like sub-layer. The SEM results obviously showed that addition of low amounts of the goethite nanoparticle increased the macrovoids formation as well as the size of the finger like macrovoids. Also, this addition decreased the skin thickness and increased the porosity of the support layer (Table I) in the blended membranes compared with that of unfilled PES membrane. The higher magnification SEM images clearly reveal these changes. The induced changes on the membranes morphology could be attributed to the interactions between components in the casting solution during the phase inversion.

According to Figure 5, the membrane prepared by adding 0.1 wt % goethite nanoparticle indicated some changes those discussed above. The produced significant changes are originated from hydrophilic nature of the goethite nanoparticle and fast exchange of solvent and nonsolvent in the coagulation bath during the phase inversion process. The same behavior was reported by some researchers for other hydrophilic nanoparticles.[10,38,39] However, a further increase of the goethite concentration (more than 0.1 wt %) reduced the pore size and porosity (Table I). By increasing the concentration of goethite, the viscosity of casting solution is increased that delay the exchange rate between solvent and nonsolvent during the phase inversion and slow down the precipitation of the membrane.[29,38] Then, the resulting membranes would be more compact and less porous compared with the fabricated membranes by less concentrations of this nanoparticle.

Surface Charge Properties of NF Membranes. One of the purposes of adding goethite nanoparticle was to endow negative charge on the PES membrane surface. In order to determine the negatively charged range of the modified PES membrane surfaces, the streaming zeta potentials of the nanocomposite PES membranes were measured. The experimental data for

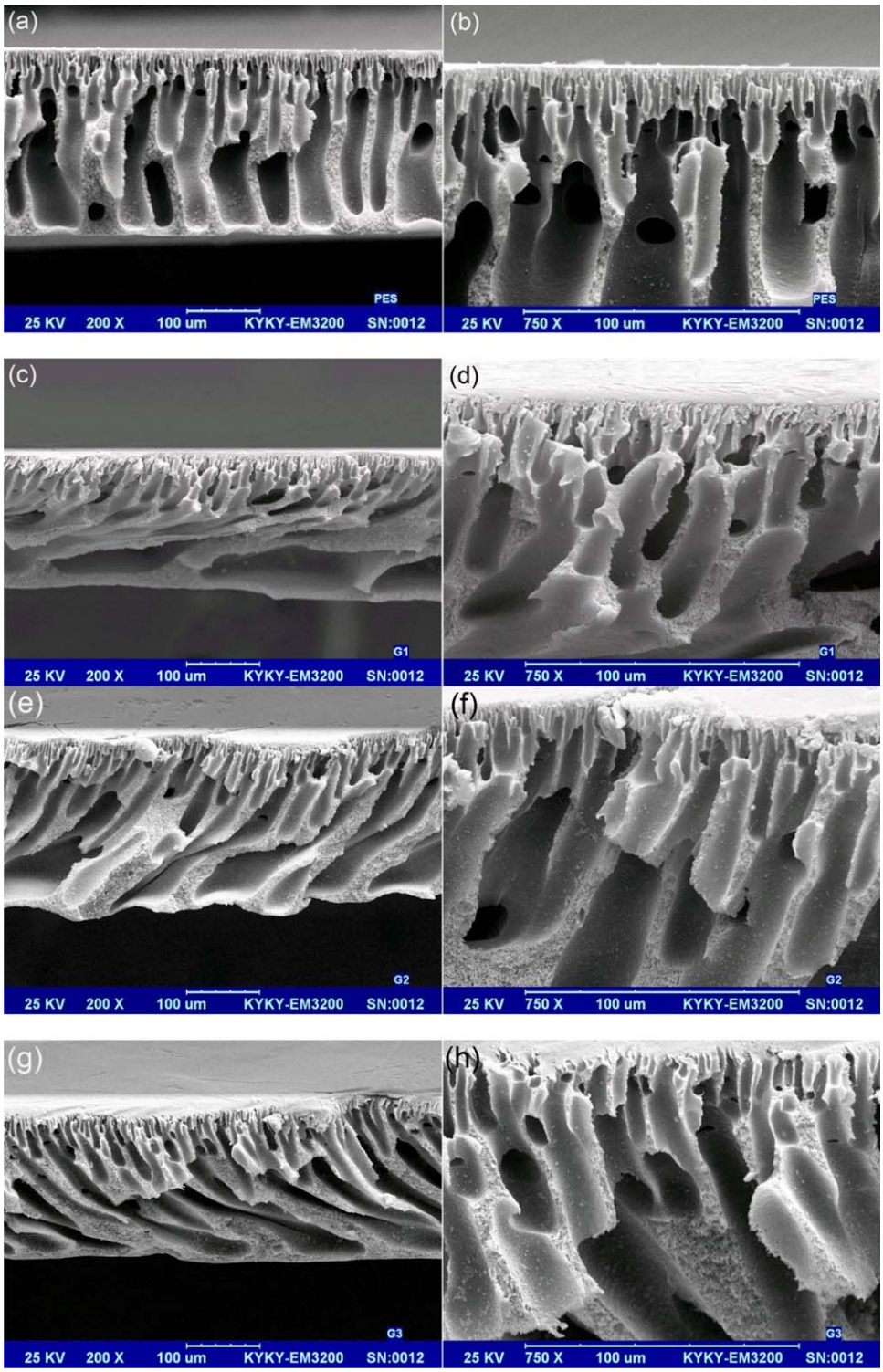

Figure 5. The cross-sectional SEM images of the prepared nanocomposite membranes (a,b) pristine PES, (c,d) 0.1 wt %, (e,f) 0.5 wt %, and (g,h) 1 wt % goethite/PES. [Color figure can be viewed in the online issue, which is available at wileyonlinelibrary.com.]

calculating zeta potentials of the prepared goethite embedded membranes and the commercial NE 4040-90 membrane in pH range of 3–8, with 1 m*M* KCl electrolyte are shown in Figure 6. The zeta potential (ζ) varies with pH of KCl solution. From these data, it could be concluded that the surface negative charge of the goethite embedded membranes increased with increase in the nanoparticles percentage.

Membrane charge creation has some procedures that adsorption of different charged solutes from electrolyte and detachment of functional groups of membrane components[40] are the most

Table I. Overall Porosity and Mean Pore Radius of the Prepared Nanocomposite Membranes

Membrane	Porosity (%)	Mean pore radius (nm)
Unfilled PES	74.3 ± 4.5	3.1 ± 0.2
0.1 wt % Goethite/PES	80.1 ± 2.7	3.8 ± 0.5
0.5 wt % Goethite/PES	79.1 ± 1.2	3.6 ± 0.3
1 wt % Goethite/PES	75.3 ± 2.9	3.3 ± 0.2

important processes. As can be seen for commercial polyamide NF membrane, it is positively charged in the lowest pH (3) and zeta potential of membrane surface decreased with pH to reach isoelectric point (5.2) and is negatively charged above this pH. However, the PES nanofiltration membranes have negative charge in the range of the examined pH. It is clear that at any pH, the absolute value of zeta potential for the high loaded membrane is lower than that of the unfilled PES membrane, which shows the goethite content has an effect on the membrane surface charge. As the content of goethite nanoparticles in casting solution increases, the number of functional groups increases and subsequently causes an improvement in negative charge density on the membrane surface.

Water Contact Angle Analysis and Pure Water Flux. Measuring water contact angle is a convenient way to assess the hydrophilic/hydrophobic property of membrane surface, which implies on the interaction energy between the surface and liquid.[10,11,41] Hydrophilicity is one of the most important properties of membranes which could influence the flux and antifouling ability of the membranes. As shown in Figure 7, after embedding of hydrophilic nano-goethite into PES membranes matrix, the water contact angles decreased. The unfilled PES membrane had the highest contact angle of almost 64.4°, corresponding to the lowest surface hydrophilicity. It can be found that the relative water contact angles decreased with the increase in nano-goethite concentration. The increase in hydrophilicity can be attributed to the spontaneous migration

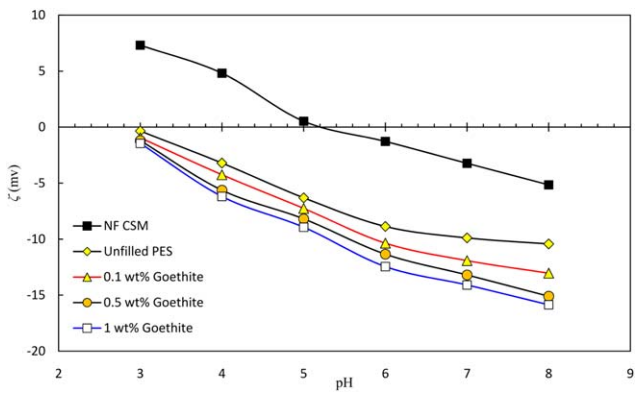

Figure 6. Zeta potential (ζ) of the nano-goethite embedded PES membranes and NE4040-90 membrane against pH with 1 m*M* KCl solution. [Color figure can be viewed in the online issue, which is available at wileyonlinelibrary.com.]

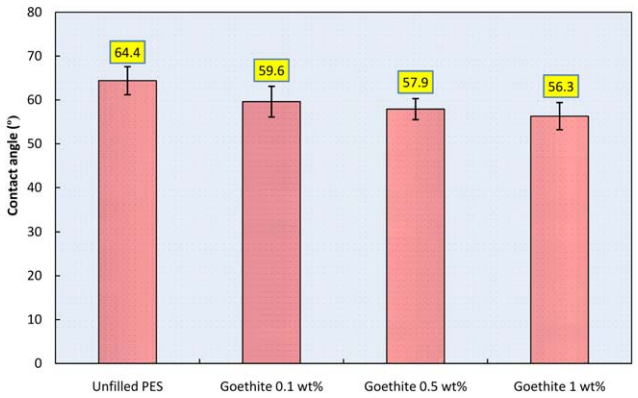

Figure 7. Static water contact angle of the prepared nano-goethite/PES membranes. [Color figure can be viewed in the online issue, which is available at wileyonlinelibrary.com.]

of hydrophilic goethite nanoparticle in the casting solution to the top surface of the prepared MMMs to reduce the interface energy during the phase inversion preparation. When the casted polymeric film on glass was immersed in non-solvent bath (water), first place contacted with the water is the air side of the casted film, which will form the membrane surface. The hydrophilic nanoparticles are tendency to the water, and therefore start to move to the water, which is penetrated from the membrane surface. Consequently, after solidification of the membranes, the most of the hydrophilic nanoparticles are located in the membrane surface. This phenomenon resulted in a hydrophilic functional groups-rich membrane surface. The images of the membranes surface are shown in Figure 8. This is in agreement with the previous observations,[11,41] in which the static contact angle declined considerably with addition of the graphene oxide and boehmite nanofillers.

In order to investigate the effects of existence of nano-goethite on performance of the prepared MMMs, pure water flux of the membranes was measured. The pure water fluxes of unfilled and blended membranes are shown in Figure 9. The results show that all of the modified membranes had higher flux relative to the unfilled PES. Adding goethite nanoparticles with hydroxyl functional groups led to the formation of hydrogen bonds between hydrogen atoms of goethite and oxygen atoms of PES polymer chains. Indeed, the generated interface area between the nanoparticles and the polymer matrix in skin layer can act as a nano-channel for diverting water through the membrane. Also, the hydrophilic properties of goethite nanoparticle can improve the hydrophilicity of membrane surface and enhance the water permeability by attracting water molecules inside the channels and facilitate them to pass through the membrane.[42] The dispersion of the hydroxylated nanoparticles inside the PES membrane is schematically shown in Figure 10. The hydrophilic particles with more water adsorption facilitate higher water permeation across the membrane pores.

Figure 9 also shows that 0.1 wt % of goethite nanoparticle/PES membrane had the highest water flux among the prepared membranes and commercial CSM NF membrane. The results showed that using high concentrations of the goethite nanoparticles (more than 0.1 wt %), the water flux decreased although

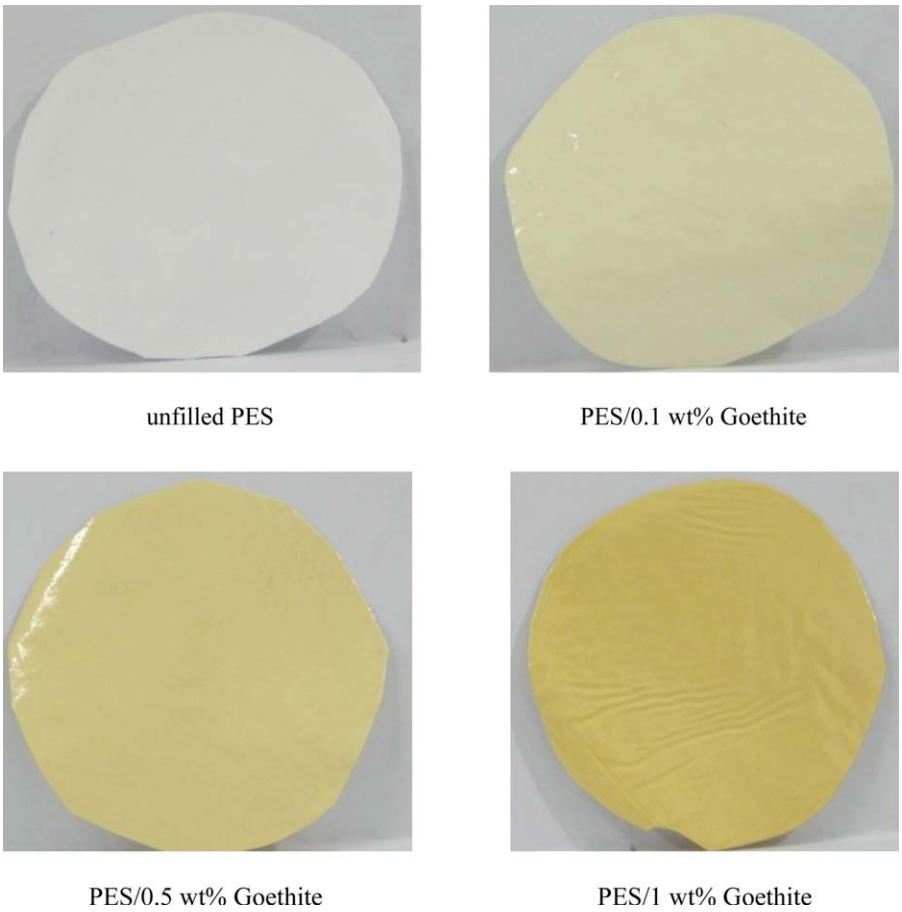

Figure 8. Digital photographs of surface of goethite embedded PES membranes with different concentrations. [Color figure can be viewed in the online issue, which is available at wileyonlinelibrary.com.]

the hydrophilicity was improved. This was because of the adverse effect of high concentrations of the nanoparticles that tend to agglomerate and plugging the membrane pores. The agglomeration of nano-goethite particles in the surface of blended membranes is depicted in Figure 11. The SEM images indicate more agglomeration at high concentrations of the nanoparticle. This behavior was similar to those reported in the earlier related works published elsewhere.[10,11,41]

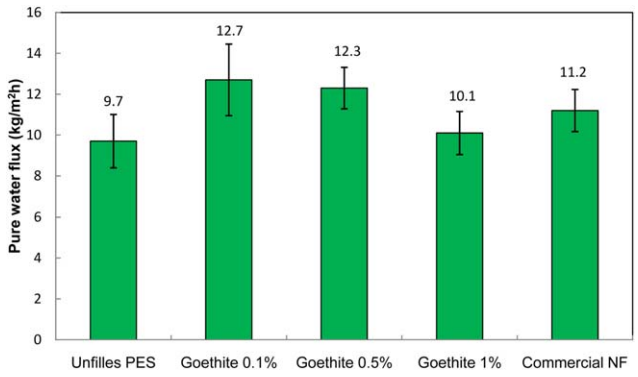

Figure 9. Pure water flux of the membranes at 4 bar (the average of three replicates was depicted). [Color figure can be viewed in the online issue, which is available at wileyonlinelibrary.com.]

In order to explain the low water flux obtained for the membranes with high hydrophilicity, bulk porosity, and mean pore radius of the MMMs were measured. Considering the data

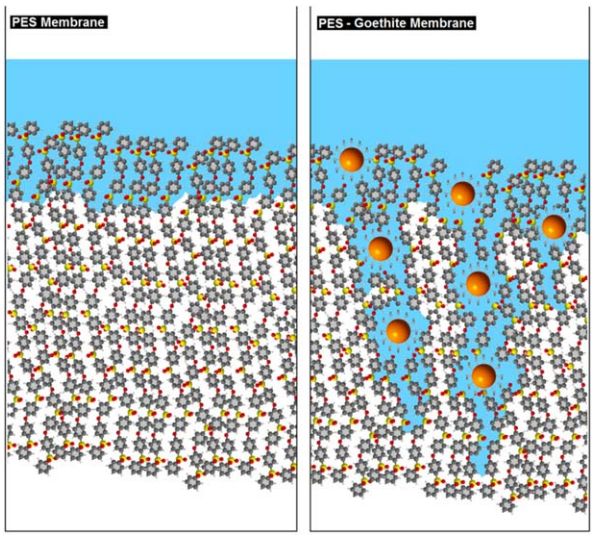

Figure 10. Schematic of interaction between nano-goethite/PES polymers in membrane matrix. [Color figure can be viewed in the online issue, which is available at wileyonlinelibrary.com.]

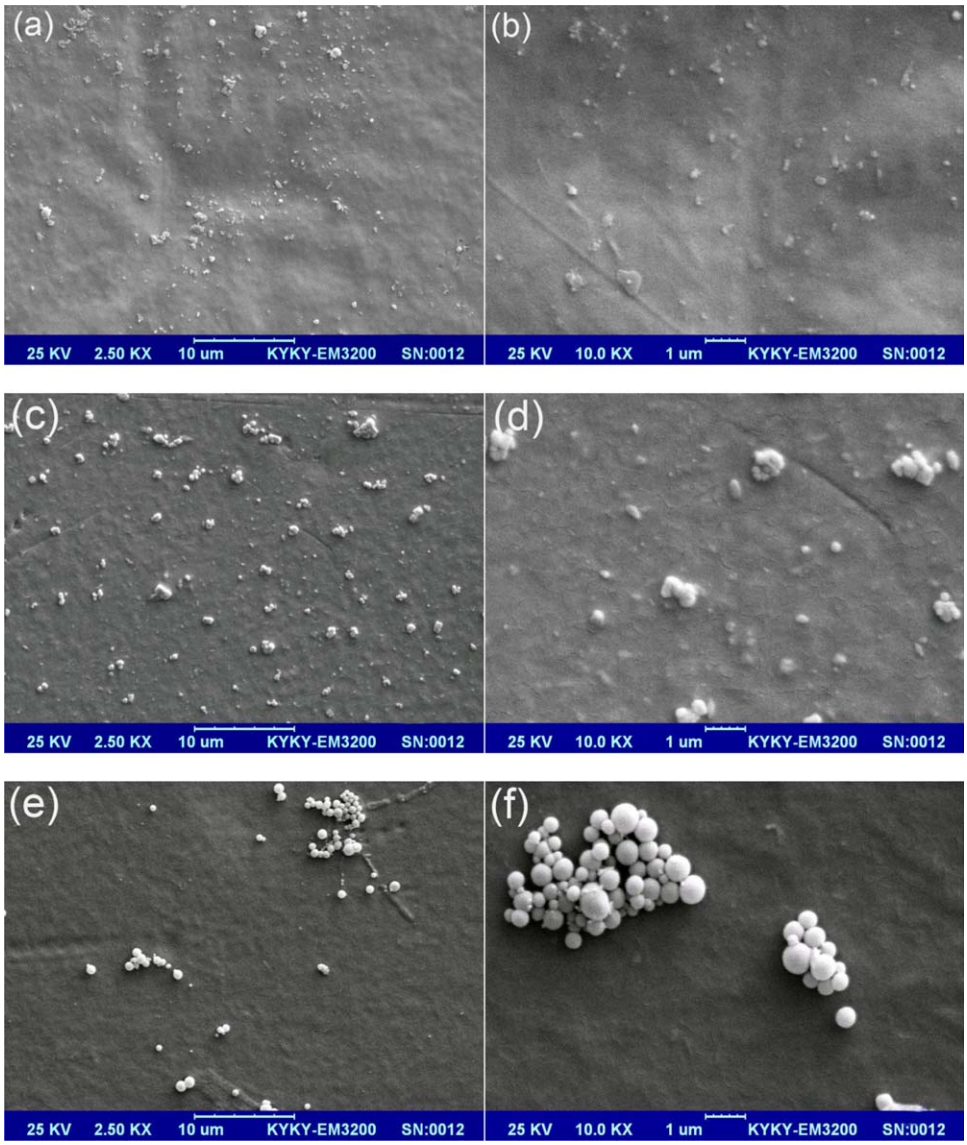

Figure 11. Dispersion and agglomeration of goethite nanoparticles in polyethersulfone matrix with two magnifications of 2500 (left) and 10,000 (right); (a,b) 0.1 wt %, (c,d) 0.5 wt %, and (e,f) 1 wt %.[Color figure can be viewed in the online issue, which is available at wileyonlinelibrary.com.]

tabulated in Table I, an increase in porosity and mean pore radius was observed for all modified membranes compared with the unfilled PES. The hydrophilic property of the goethite nanoparticles caused an increase in the solution thermodynamic instability in the gelation bath. Consequently, it resulted in an increase in solvent and nonsolvent exchange rate during membrane formation that leads to higher porosity and pore radius in the membrane surface as well as improves the water permeability.[10,11] As shown in Table I, using high concentrations of the goethite nanoparticles (more than 0.1 wt %) lead to a decrease in porosity and pore radius. This might be related to increase in viscosity of the blend solution because of addition of the nanoparticles.[10,11] Increase in solution viscosity usually delays the exchange of solvent and nonsolvent. This suppresses the formation of macro-voids (see cross-sectional SEM images) and reduces the membrane porosity. In addition, agglomerations of goethite nanoparticles caused clogging of the membranes pores and reduced the mean pore radius of the membrane, as presented in Table I. The observed trend for the mean pore radius was very well matched with the water flux through the membranes, suggesting that the pure water flux was also affected by the membranes pore sizes. Nevertheless, addition of any goethite nanoparticle into membrane matrix resulted in considerably higher porosity and pore radius in comparison with unfilled PES membrane. The results showed that water flux of the membranes could be controlled by hydrophilicity and pore size. By increasing in hydrophilicity and pore size, water permeation through the membranes is increased. However, one of the factors can have dominant effect sometimes. In this study, although the hydrophilicity of 0.5 and 1 wt % goethite membrane were higher than that of 0.1 wt % membrane, their pure water fluxes were lower because of reduction in pore size and porosity.

Figure 12. The photos of (a) feed solution, (b) permeation from PES/0.1 wt % goethite membrane (c) permeation from unfilled PES membrane. [Color figure can be viewed in the online issue, which is available at wileyonlinelibrary.com.]

Nanofiltration Performance and Dye Removal Capability. A series of experiments were carried out for evaluation of colored wastewater treatment using the prepared NF membranes. Figure 12 shows images of feed solution and permeates from unfilled PES and 0.1 wt % goethite-embedded PES membranes. As shown in this figure, the goethit- embedded membrane permeate is quite clear, but unfilled PES membrane permeate has a darker color, indicating lower dye rejection. The results of dye rejection are presented in Figure 13. This figure demonstrates the capability of the prepared membranes for Direct Red 16 removal from synthetic feed (30 mg/L) after 60 min filtration as a function of goethite amount in the casting solution.

The rejection was increased with addition of goethite nanoparticles in the casting solution. All dye rejection values of the blended membranes were higher than 98%, which meant that the goethite–PES membranes retained a desirable nanofiltration property.

In nanofiltration process, two mechanisms of Donnan exclusion and steric hindrance (molecular sieving) are generally concluded with the solute retention.[43] The Donnan exclusion is connected

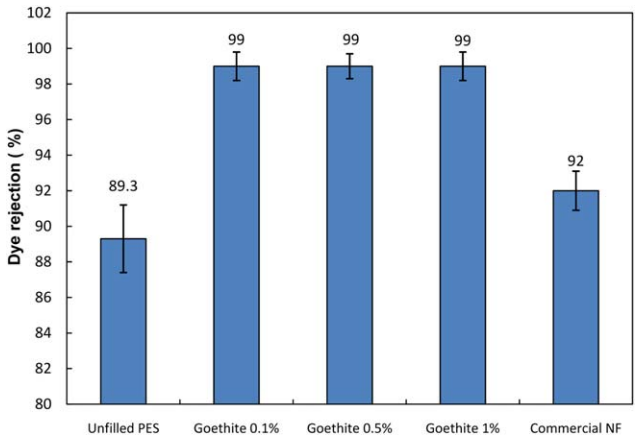

Figure 13. Dye retention performance of the prepared goethite/PES nanofiltration membranes (4 bar, pH = 6.0 ± 0.1, 30 mg/L Direct Red 16, after 60 min filtration). [Color figure can be viewed in the online issue, which is available at wileyonlinelibrary.com.]

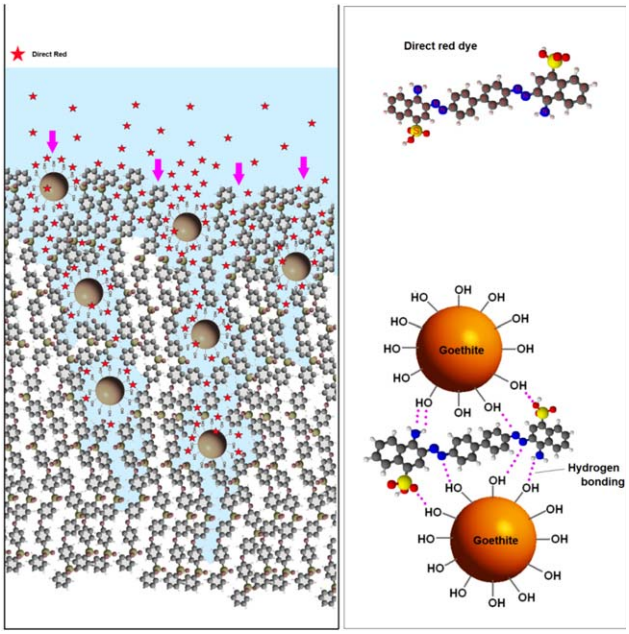

Figure 14. Interaction between Direct Red 16 and nano-goethite in the matrix of the prepared membranes. [Color figure can be viewed in the online issue, which is available at wileyonlinelibrary.com.]

to the membrane surface charge and the steric hindrance is associated to the membrane pore size.

The mean pore radius of the nano-goethite mixed membranes is higher than the unmodified membrane (see Table I). However, their rejection is quite better. This is because of more negative charge of the goethite-embedded membranes (see Figure 6 related to zeta potential) resulted from presence of hydroxyl groups on the surface of nano-goethite particles that induced their charge to the membrane surface and cause supremacy of Donnan exclusion mechanism related to steric hindrance (molecular sieving). This indicates that Donnan exclusion (electrostatic repulsion) was more predominant than the steric factors for these MMMs in the separation of dye.

Another mechanism for explaining high rejection of the dye by MMMs can be sorption/adsorption of the dye by goethite nanoparticle. The functional groups of Direct Red 16 such as $–NH_2$, $–SO_3H$, and –OH can be interacted by hydroxyl groups of the nano-goethite. This interaction is hydrogen bonding, which results in adsorption of the dye by membrane surface and membrane inside pore structure, as schematically shown in Figure 14. This adsorption leads to higher rejection characteristics of the nanocomposite membranes. This adsorption mechanism can be approved by visual investigation of the tested membranes. Figure 15 presents the surface photograph images of the modified and unfilled membranes. From this figure one can see that the color of the nano-goethite filled membrane is darker than the unfilled membrane, showing more adsorption of the dye on the surface of the modified membrane. This means that there are interactions between the dye and the MMMs.

As shown in Figure 16, the permeate flux of dye solution had the same trend as pure water flux as a function of nano-

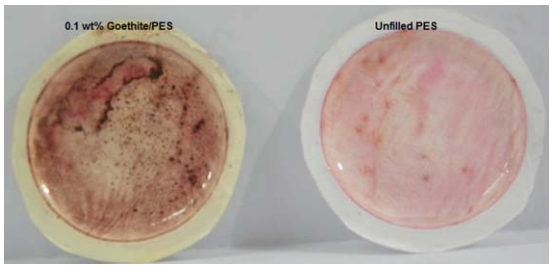

Figure 15. Digital camera images of the membranes after filtration of Direct red 16. [Color figure can be viewed in the online issue, which is available at wileyonlinelibrary.com.]

goethite concentration. However, the flux of dye solution permeate was slightly lower than that of pure water because of fouling effect of the dye. However, this reduction in flux was very low, indicating good antifouling properties of the prepared membranes.

Antifouling Properties

Figure 17 shows the time-dependent permeate flux for PES membrane and different composites of goethite-PES membranes. The corresponding flux recovery ratio and fouling resistance ratio values are presented in Figure 17. In this study, 8000 ppm of powder milk solution (for simulating protein solution) was used for fouling experiments. It can be clearly seen that, the modified membranes showed relatively better antifouling properties than those of the unmodified membrane. The improvement of hydrophilic properties agrees with enhancement of antifouling performance.[10,11] While the membrane modification showed increased antifouling performance at 0.1 wt % goethite, at higher concentrations, the modifications may not be sufficient to prevent agglomeration.[38]

Flux recovery ratio (*FRR %*), reversible resistance (R_r), irreversible resistance (R_{ir}), and total filtration resistance (R_t) were calculated by eqs. (4–7). The reversible resistance is because of loose attachment of foulants on the membrane surface, while the irreversible resistance is because of adsorption of foulants on membrane pore wall or surface.[11] As can be seen in Figure

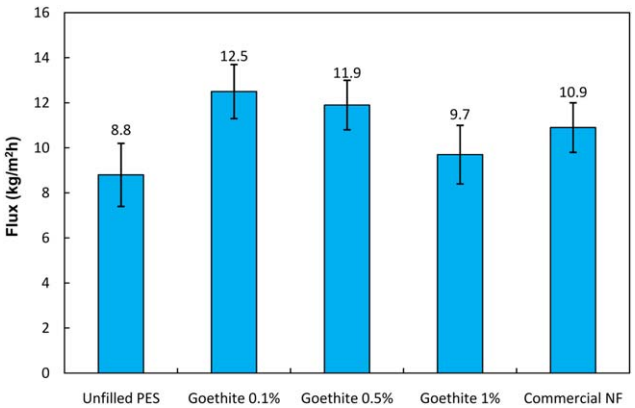

Figure 16. Permeate flux of Direct red 16 solution with concentration of 30 mg/L at 4 bar during 60 min as a function of the nano-goethite content. [Color figure can be viewed in the online issue, which is available at wileyonlinelibrary.com.]

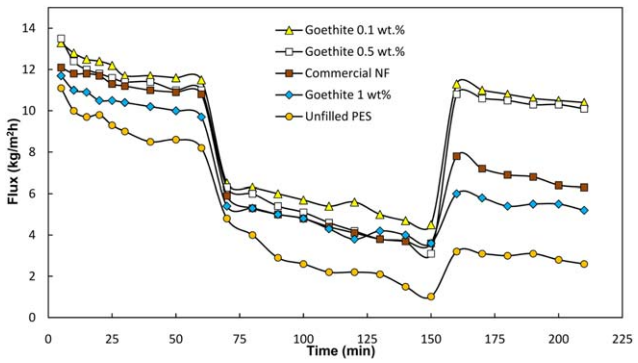

Figure 17. Flux versus time of the membranes at 4 bar during three steps: water flux (60 min), powder milk solution (90 min), and water flux (60 min) after 15 min washing with distilled water. [Color figure can be viewed in the online issue, which is available at wileyonlinelibrary.com.]

18, when the content of the goethite nanoparticle in the casting solution increased from 0 to 0.1 wt %, the *FRR* increased from 35% to 87.5%. This suggests that the adsorption between protein and blended membranes was weaker than adsorption between protein and pure PES membrane. Therefore, the foulant stuck in a lesser amount in the more hydrophilic membrane surface and could be more easily washed off from the surface.[42,44] The goethite embedded membranes have better antifouling properties compared to the commercial CSM NF membrane.

The results also showed that the irreversible resistance significantly decreased by addition of nano-goethite in casting solution up to 0.1 wt %. Further addition of goethite in the casting solution caused an increase in membrane resistance. This might be a consequence of precipitation of goethite nanoparticles during the casting and phase inversion process, which causes pore plugging and provides extra hydraulic resistance.[41] The SEM images, shown in Figure 11, approve these results.

Also, the *FRR* of the prepared nanocomposite membranes was tested by filtration of the dye solution and the results were

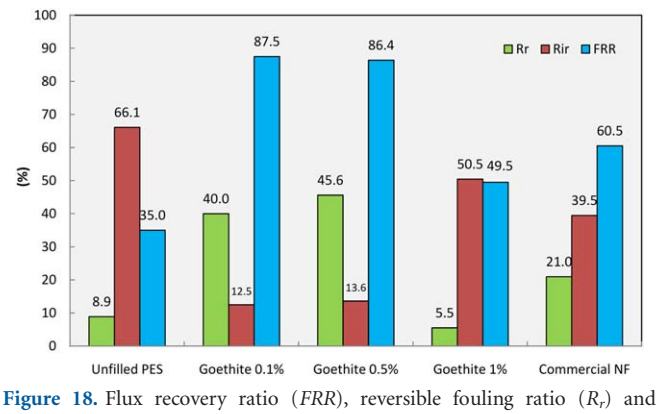

Figure 18. Flux recovery ratio (*FRR*), reversible fouling ratio (R_r) and irreversible fouling ratio (R_{ir}) of the prepared nanocomposite membranes and commercial CSM NF membrane in filtration of powder milk solution. [Color figure can be viewed in the online issue, which is available at wileyonlinelibrary.com.]

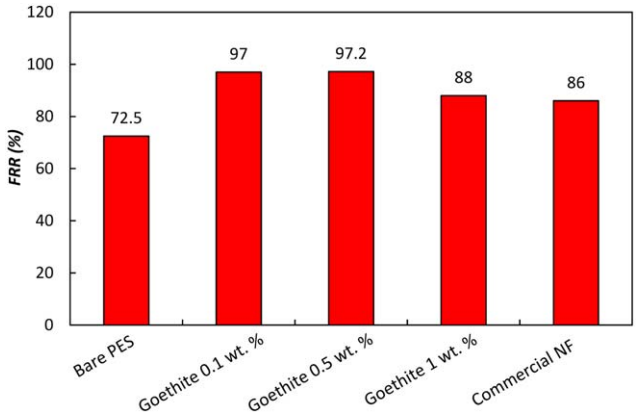

Figure 19. *FRR* of the membranes in filtration of Direct red 16 dye solution. [Color figure can be viewed in the online issue, which is available at wileyonlinelibrary.com.]

depicted in Figure 19. As shown, the *FRR* value in the presence of the dye solution is higher than the milk powder solution; presenting this fact that the fouling capability of the Direct red 16 dye is lower than the protein solution. Therefore, the prepared membranes could effectively apply in textile wastewater treatment.

CONCLUSIONS

In the present study, a hydrophilic additive, goethite nanoparticle, was successfully synthesized and incorporated in to the matrix of PES membrane during the nonsolvent induced phase inversion to improve membrane flux and antifouling performance. The influence of nano-goethite contents in the casting solution were investigated and optimized, resulting in the optimal nanoparticle concentration of 0.1 wt %. The fabricated MMMs showed higher flux and dye rejection of 99% rather than unmodified membranes. However, the high amount of the nanoparticle caused a decrease in the water flux. By embedding of the nano-goethite, hydrophilicity of the nanocomposite membranes was improved. Interactions between the dye and the goethite nanoparticles in the MMMs caused a high rejection because of adsorption of the dye on the surface of the modified membranes. Antifouling experiments showed that adding goethite nanoparticle in the casting solution lead to increase of flux recovery from 0 to 0.1 wt % and decrease in irreversible fouling from 66.1 to 12.5 wt % compared with the unfilled membrane.

ACKNOWLEDGMENTS

The authors gratefully acknowledge the financial support by the Iran National Science Foundation (INSF) (Grant no. 91055010).

REFERENCES

1. Brik, M.; Schoeberl, P.; Chamam, B.; Braun, R.; Fuchs, W. *Process Biochem.* **2006**, *41*, 1751.
2. Vandevivere, P. C.; Bianchi, R.; Verstraete, W. *J. Chem. Technol. Biotechnol.* **1998**, *72*, 289.
3. Terras, C.; Vandevivere, P.; Verstraete, W. *Water Sci. Technol.* **1999**, *39*, 81.
4. Delee, W.; O'Neill, C.; Hawkes, F. R.; Pinheiro, H. M. *J. Chem. Technol. Biotechnol.* **1998**, *73*, 323.
5. Sevimli, M. F.; Kinaci, C. *Water Sci. Technol.* **2002**, *45*, 279.
6. Arslan-Alaton, I.; Seremet, O. *J. Environ. Sci. Health Part A: Toxic Hazard. Subst. Environ. Eng.* **2004**, *39*, 1681.
7. Rott, U.; Minke, R. *Water Sci. Technol.* **1999**, *40*, 137.
8. Tang, C.; Chen, V. *Desalination* **2002**, *143*, 11.
9. Aydiner, C. *J. Membr. Sci.* **2010**, *361*, 96.
10. Vatanpour, V.; Madaeni, S. S.; Rajabi, L.; Zinadini, S.; Derakhshan, A. A. *J. Membr. Sci.* **2012**, *401402*, 132.
11. Zinadini, S.; Zinatizadeh, A. A.; Rahimi, M.; Vatanpour, V.; Zangeneh, H. *J. Membr. Sci.* **2014**, *453*, 292.
12. Rahimpour, A. *Desalination* **2011**, *265*, 93.
13. Cheng, C.; Ma, L.; Wu, D.; Ren, J.; Zhao, W.; Xue, J.; Sun, S.; Zhao, C. *J. Membr. Sci.* **2011**, *378*, 369.
14. Wang, D.; Zou, W.; Li, L.; Wei, Q.; Sun, S.; Zhao, C. *J. Membr. Sci.* **2011**, *374*, 93.
15. Ba, C.; Economy, J. *J. Membr. Sci.* **2010**, *362*, 192.
16. Kim, J.; der Bruggen, B. V. *Environ. Pollut.* **2010**, *158*, 2335.
17. Zhao, C.; Xue, J.; Ran, F.; Sun, S. *Prog. Mater. Sci.* **2013**, *58*, 76.
18. Yu, S.; Zuo, X.; Bao, R.; Xu, X.; Wang, J.; Xu, J. *Polymer* **2009**, *50*, 553.
19. Li, L. H.; Deng, J. C.; Deng, H. R.; Liu, Z. L.; Xin, L. *Carbohydr. Res.* **2010**, *345*, 994.
20. Ahn, J.; Chung, W. J.; Pinnau, I.; Guiver, M. D. *J. Membr. Sci.* **2008**, *314*, 123. 314, 2008, 123.
21. Maximous, N.; Nakhla, G.; Wan, W.; Wong, K. *J. Membr. Sci.* **2009**, *341*, 67.
22. Sadeghi, M.; Semsarzadeh, M. A.; Moadel, H. *J. Membr. Sci.* **2009**, *331*, 21.
23. Hosseini, S. M.; Madaeni, S. S.; Heidari, A. R.; Amirimehr, A. *Desalination* **2012**, *284*, 191.
24. Harman, B. I.; Koseoglu, H.; Yigit, N. O.; Beyhan, M.; Kitis, M. *Desalination* **2010**, *261*, 27.
25. Daraei, P.; Madaeni, S. S.; Ghaemi, N.; Salehi, E.; Khadivi, M. A.; Moradian, R.; Astinchap, B. *J. Membr. Sci.* **2007**, *415–416*, 250.
26. Bakoyannakis, D. N.; Deliyanni, E. A.; Zouboulis, A. I.; Matis, K. A.; Nalbandian, L.; Kehagias, T. *Microporous Mesoporous Mater.* **2003**, *59*, 35.
27. Boily, J. F.; Felmy, A. R. *Geochim. Cosmochim. Acta* **2008**, *72*, 3338.
28. Zhang, L.; Chae, S. R.; Lin, S.; Wiesner, M. R. *Environ. Eng. Sci.* **2012**, *29*, 124.
29. Hackley, V. A.; Anderson, M. A. *J. Membr. Sci.* **1992**, *70*, 41.
30. Schaep, J.; Van der Bruggen, B.; Vandecasteele, C.; Wilms, D. *Sep. Purif. Technol.* **1998**, *14*, 155.
31. Smoluchowski, M. Handbook of Electricity and Magnetism; Barth: Leipzig, **1921**; Vol. *2*, p 366.
32. Abramson, H. A. *J. Phys. Chem.* **1934**, *38*, 1128.

33. Jacobasch, H. J.; Schurz, J. *Prog. Colloid Polym. Sci.* **1988**, *77*, 40.
34. Fairbrother, F.; Mastin, H. *J. Chem. Soc.* **1924**, *125*, 2319.
35. Saiena, J.; Asgari, M.; Soleymani, A. R.; Taghavinia, N. *Chem. Eng. J.* **2009**, *151*, 295.
36. Stachowicz, M.; Hiemstra, T.; van Riemsdijk, W. H. *J. Colloid. Interface Sci.* **2008**, *320*, 400.
37. Kugbe, J.; Matsue, N.; Henmi, T. *J. Hazard. Mater.* **2009**, *164*, 929.
38. Arthanareeswaran, G.; Sriyamuna Devi, T. K.; Mohan, D. *Sep. Purif. Technol.* **2009**, *67*, 271.
39. Yu, L. Y.; Xu, Z. L.; Shen, H. M.; Yang, H. *J. Membr. Sci.* **2009**, *337*, 257.
40. Gherasim, C.; Cuhorka, J.; Mikulasek, P. *J. Membr. Sci.* **2013**, *436*, 132.
41. Vatanpour, V.; Madaeni, S. S.; Moradian, R.; Zinadini, S.; Astinchap, B. *J. Membr. Sci.* **2011**, *375*, 284.
42. Yang, Y.; Wang, P.; Zheng, Q. *J. Polym. Sci. Polym. Phys.* **2006**, *44*, 879.
43. Maurya, S. K.; Parashuram, K.; Singh, P. S.; Ray, P.; Reddy, A. V. R. *Desalination* **2012**, *304*, 11.
44. Razmjou, A.; Mansouri, J.; Chen, V. *J. Membr. Sci.* **2011**, *378*, 73.